Geochimica et Cosmochimica Acta Vol. 52, pp. 1615–1626

0016-7037/88/$3.00 + .00

Murchison xenoliths

EDWARD J. OLSEN[1,6], ANDREW M. DAVIS[2], IAN D. HUTCHEON[3], ROBERT N. CLAYTON[4,5,6], TOSHIKO K. MAYEDA[4] and LAWRENCE GROSSMAN[4,6]

[1]Field Museum of Natural History, Chicago, IL 60605, U.S.A.
[2]James Franck Institute, University of Chicago, Chicago, IL 60637, U.S.A.
[3]Division of Geological and Planetary Sciences, California Institute of Technology, Pasadena, CA 91125, U.S.A.
[4]Enrico Fermi Institute, University of Chicago, Chicago, IL 60637, U.S.A.
[5]Department of Chemistry, University of Chicago, Chicago, IL 60637, U.S.A.
[6]Department of Geophysical Sciences, University of Chicago, Chicago, IL 60637, U.S.A.

(*Received August* 24, 1987; *accepted in revised form March* 11, 1988)

Abstract—C3 xenoliths in a C2 host (Murchison) are unique among known meteoritic xenolith-host occurrences. They offer an opportunity to determine possible effects on the xenoliths by the hydrated host. Eleven xenoliths were found ranging from 2 to 13 mm. Four of these Murchison Xenoliths (MX1, MX2, MX3 and MX4) have been studied in detail. MX1 and MX2 were large enough for trace element, oxygen isotope, carbon isotope, bulk carbon and bulk nitrogen determinations. All four were studied petrographically and by analytical SEM. The xenoliths cannot be unequivocally identified as C3V or C3O subtypes. MX1 contains some matrix phyllosilicate, indicating reaction with water. MX1, MX2 and MX3 all show extensive alteration by an FeO-rich medium, and some minerals in them contain ferric iron. MX4, however, exhibits very minor alteration by FeO only. Oxygen isotopic and chemical data show that the alteration of these xenoliths did not take place in the Murchison host. The alterations occurred in one or more parent bodies, which were later disrupted to release these xenoliths that ultimately accreted onto the Murchison parent body.

INTRODUCTION

UNDERSTANDING EARLY STAGES of asteroid and planet formation in the Solar System is one aim of current meteorite-based space research. How the processes took place is subject to modelling, but any model must ultimately be in accord with physical observations. Evidence accrues from many approaches; one approach examines host/clast relationships among polymict accretionary breccias, which is the subject of this paper.

The literature on this subject continues to grow. Basic observations from this literature are listed in Table 1, which summarizes many, but not necessarily all published host/clast occurrences. Analyses of these occurrences have led workers to conclude that some xenoliths underwent metamorphic processing or alteration in their own parent bodies, which were then fragmented, partly or completely, to be reassembled as gravitationally-bound rubble, or added to the growing regoliths of less disturbed asteroids (TAYLOR *et al.*, 1987; NOZETTE and WILKENING, 1982; KRACHER *et al.*, 1985; ARMSTRONG *et al.*, 1982).

Each different combination of xenolith and host adds detail to the emerging picture of those early "days". Although the data base is not large (relative to the total of known meteorites), a common feature in Table 1 is the occurrence of C2 xenoliths in a variety of host types. The unique occurrence is the presence of obvious C3 xenoliths in a C2 host (FUCHS *et al.*, 1973).

FUCHS *et al.* (1973) reported six C3 clasts within the Murchison C2 chondrite. Since that time we have discovered five more such clasts in Murchison. These are designated MX (Murchison Xenoliths) and are numbered MX1 through MX11. In hand specimen these clasts are pale gray to dark gray and stand out against the black color of the host (Fig. 1). Four of them, MX1–4, were selected for this work. MX1 and MX2 were chosen because they are the largest (long dimensions of 13 mm and 5.5 mm, respectively) and could be sampled for several kinds of measurements. MX3 and MX4 (long dimensions of 2.3 mm and 2.0 mm, respectively) were randomly selected from the remaining nine (all in the range of 2–3 mm). The xenoliths do not have especially rounded outlines; most, in fact, are obviously angular chips. They show sharp contacts and no sign of interaction with the surrounding Murchison host. None of the xenoliths has rims.

Because of its size, more detail was obtained from MX1 than from any other xenolith. To avoid repetition, MX1 will be used as a reference, and described more fully. The other xenoliths will be described relative to it, primarily emphasizing differences and similarities with MX1.

METHODS OF STUDY

Energy dispersive analyses (EDS) were done on polished sections on a JEOL JSM-35 scanning electron microscope (SEM) equipped with a Kevex EDS system. Data were reduced on-line using a ZAF-MAGIC V algorithm (J. W. COLBY, Kevex Corp.) with both mineral and synthetic glass standards. Data were collected at 15 KV and 150 pA with 200 sec. counting times. Based on analyses of minerals of known compositions, results are accurate to 3% relative to the amounts present; precision is better than 1%.

Analyses of oxide minerals in MX1–3 gave high cation totals when all Fe was reported as FeO. Under the same analytical operating conditions, analyses of oxide minerals in MX4 did not give high cation totals. It appeared that some portion of the iron in oxide minerals in MX1–3 was present as ferric iron, while all iron in MX4 was ferrous. Analyses in MX1–3 were recomputed to satisfy stoichiometry by calculating a portion of the FeO as Fe_2O_3. To check this practice further, standards of spinel group minerals were sought that had been analyzed for ferrous and ferric iron by wet chemical methods. Many such standards exist, however, on the spatial level of an EDS analytical system the ferric iron is often strongly zoned so that any individual grain may or may not have the ferric iron content of the large bulk that was analyzed by wet chemistry (I. M. STEELE, pers. commun.). To circumvent this, several dozen grains of each of four wet chemically

Table 1. Xenoliths in meteorites.

Xenolith type	Host type	Reference
Carbonaceous	H	RUBIN *et al.* (1983)
C2	C3	KRACHER *et al.* (1985)
C2	H	NOZETTE and WILKENING (1982)
C2	Howardite	BUNCH *et al.* (1976)
C2	Howardite	WILKENING (1973)
C2, H	H	FODOR and KEIL (1976)
C3	C2	FUCHS *et al.* (1973)
C3	C3	KURAT *et al.* (1987)
CAI	H, L, LL	BISCHOFF and KEIL (1983)
CAI	E	BISCHOFF *et al.* (1985)
Anom. chondrite	LL	RUBIN *et al.* (1982)
Chondrules	Howardites	OLSEN *et al.* (1987)
LL	H	RUBIN *et al.* (1983)
LL	Mesosiderite	KALLEMEYN *et al.* (1978)
H	LL	DODD (1974)
H	L	MAYEDA *et al.* (1986)
Achondrite	L	HUTCHISON *et al.* (1986)
Eucrite	Eucrite	MIYAMOTO *et al.* (1979)
Eucrite	Eucrite	OLSEN *et al.* (1978)
Unknown type	C2	FUCHS *et al.* (1973)
Cristobalite	L	BINNS (1967)
Cristobalite	L	OLSEN *et al.* (1981)
Cristobalite	H	CHRISTOPHE MICHEL-LEVY and CURIEN (1965)

analyzed standards were selected. EDS analyses were made of at least 8 to 15 grains of each of these. The results for each were averaged. In each case the cation totals were high when the all iron was reported as FeO. Ferric iron was calculated to satisfy stoichiometry and plotted against ferric iron reported in the wet chemical analyses, constraining the plot to pass through the origin, as it must. The regression gave a slope of 0.98 with a linear correlation coefficient of 0.93. Based on this, as well as analyses of MX4 oxides on the same analytical instrument, we conclude that the calculated ferric iron contents in MX1–3 oxide minerals are real, and, as discussed later, that MX4 has not undergone significant oxidation.

Neutron activation analyses were performed on MX1 and MX2 by the method reported by L. GROSSMAN *et al.* (1981).

Oxygen isotope analyses on MX1 and MX2 were performed by the method described by CLAYTON and MAYEDA (1963).

Bulk nitrogen, bulk sulfur and carbon isotope analyses on MX1 and MX2 were performed by the method described by HALBOUT *et al.* (1986).

Infrared spectrometry was performed on MX1 over the range 4200 to 250 cm^{-1} using a Perkin-Elmer Model 180 IR spectrometer. Chips of MX1 were ground; 1 mg samples were mixed with 180 mg of dried, spectrographic grade KBr and pelletized. The pellets were stored in a desiccator and the spectrometer was purged with dry nitrogen during acquisition of spectra.

Ion microprobe analysis for hydrogen in MX1 was performed on a modified AEI-20 instrument (BANNER and STIMPSON, 1975) following procedures by STEELE *et al.* (1981).

X-ray powder diffraction data were collected on a 114 mm diameter camera using Fe radiation with 9 hour exposures.

PETROGRAPHY AND MINERAL CHEMISTRY OF CLASTS

FUCHS *et al.* (1973) determined that MX1 is a C3 chondrite with characteristics of both the C3V and C3O subtypes. Later in this paper we show that the $\partial^{18}O$ (SMOW) and $\partial^{13}C$ (PDB) values for MX1 and MX2 fall together and are far outside the C1 and C2 chondrite ranges.

The next question is whether these clasts are a mixture of C3V and C3O subtypes, or all of one subtype. VAN SCHMUS (1969) originally characterized these two subtypes and MCSWEEN (1977) and RUBIN (1984) have proposed additional criteria. MX1 and MX2 are large enough to be representative of their parent material; MX3 and MX4 (as well as MX5–11) are, however, too small to be representative. Thus, for MX3 and MX4 it is not possible to answer this question.

MX1 (13.0 × 12.8 mm)

MX1 is separated from its host by a thin crack. In thin section this xenolith has relatively large inclusions (chondrules, mineral fragments, aggregates), abundant opaque matrix, abundant sulfide (1–100 μm grains) and, except for a few submicrometer grains, is essentially metal-free. The sulfide is mainly troilite with about 5 vol% pentlandite. Based on the criteria of VAN SCHMUS (1969) these features suggest that MX1 is a C3V. On the other hand, the matrix is more similar in texture to the grain sizes and shapes of the C3O, Ornans, and unlike the type C3V, Vigarano (Fig. 2). MCSWEEN (1977) determined that the matrix/inclusion ratio is near 2 for C3V and 0.5 for C3O chondrites. A point count of MX1 gives a ratio of 1.9, like a C3V. Finally, RUBIN (1984) found that coarse grained rims occur around ≈50% of the inclusions in the C3V subtype and <1% in the C3O subtype. Coarse-grained rims were not found around any inclusions in MX1, suggesting that it is like a C3O. Thus, by two criteria MX1 is a C3O, and two other criteria indicate it is a C3V. It appears that MX1 cannot be put unequivocally into either of these categories.

MX1 inclusions. Most inclusions in MX1 are unremarkable in that they are petrographically and mineralogically similar to inclusion types well known in C3 chondrites. A few inclusions, however, are notable in what they reveal about the history of MX1.

Inclusion MX1/A (120 × 200 μm; Fig. 3) is a loosely consolidated aggregate of irregularly-shaped iron-rich spinel grains with minor hibonite blades, 2–10 μm long (Table 2), poikilitically enclosed within the spinel. It is surrounded by a convoluted rim, 2–5 μm thick, of blocky, 1–3 μm, calcic pyroxene grains (Table 3). Spinel grains are all enriched in iron towards their edges (15.9–32.7 wt% FeO, core to rim). Also poikilitically enclosed in spinel are rare grains of perovskite and ilmenite. One such inclusion (2 × 4 μm ellipse) is

FIG. 1. Macroscopic view of MX1 xenolith (13 mm diam.). The xenolith stands out sharply against the Murchison matrix.

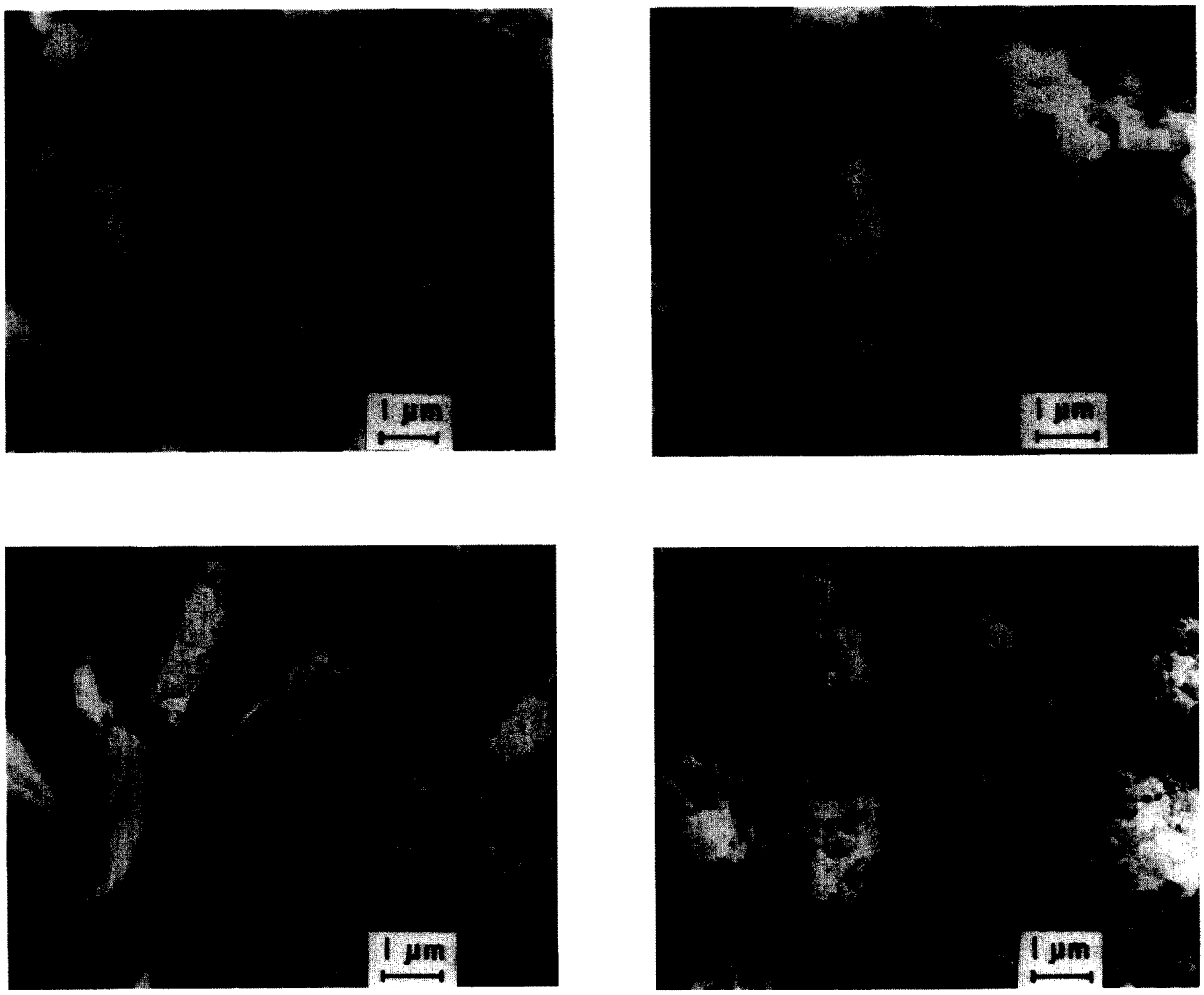

FIG. 2. Secondary electron images of matrices of carbonaceous chondrites on broken surfaces. All photographs taken at same magnification (originally 10,000×). a. MX1; b. Ornans; c. Allende; d. Vigarano. The matrices of the MX xenoliths most closely resemble Ornans matrix in grain size and morphology.

perovskite at one end and ilmenite at the other end. A fracture in the spinel leads to the ilmenite end, suggesting the ilmenite formed by reaction of perovskite with an iron-rich agent. Ilmenite analyses give high cation totals when all iron is reported as FeO; calculation based on stoichiometry shows the presence of some trivalent iron (Table 2). Similarly, spinel analyses indicate the presence of ferric iron (Table 2).

Inclusion MX1/B (40 × 60 μm; Fig. 4) consists mainly of two large (25 μm) iron-rich spinel grains (21.0–25.4 wt% FeO) (Table 2) surrounded by a diopside (He3) rim (Table 3). Within the spinel crystals are grains of perovskite and ferric iron-bearing titanomagnetite, the latter containing 72 mole percent ulvöspinel.

Inclusion MX1/C (120 × 260 μm; Figs. 5, 6) is a mosaic of whitlockite, calcic pyroxene, pentlandite, chromian magnetite (Table 2) and fayalitic olivine grains surrounding a core consisting of 2–10 μm calcic pyroxene grains. Each grain of pyroxene in the outer mosaic has a core of enstatite (Table 3) surrounded by iron-bearing salite (Table 3) and a rim of olivine, ≈Fa50. Cr-magnetite grains are sometimes rimmed by Cr-free magnetite. A few beads of Ni-rich metal (61–74 wt% Ni), up to 1 μm, occur within whitlockite.

MX1/C resembles the metal-sulfide-phosphate inclusions described by RAMBALDI and RAJAN (1982) in the type 3 ordinary chondrites, Chainpur and Krymka. It is similar to, but morphologically and mineralogically more complex than the phosphate-sulfide inclusions in C3 meteorites described by RUBIN and J. GROSSMAN (1985). It bears a resemblance to some Fremdlinge in C3 chondrites (EL GORESY *et al.*, 1978), however, no refractory metal nuggets or vanadium-rich phases were found in it.

Inclusion MX1/D (80 μm diam.; Fig. 7) is an aggregate of grains, the center of which consists of irregularly shaped fassaite grains with minor Fe-rich spinels. The entire inclusion

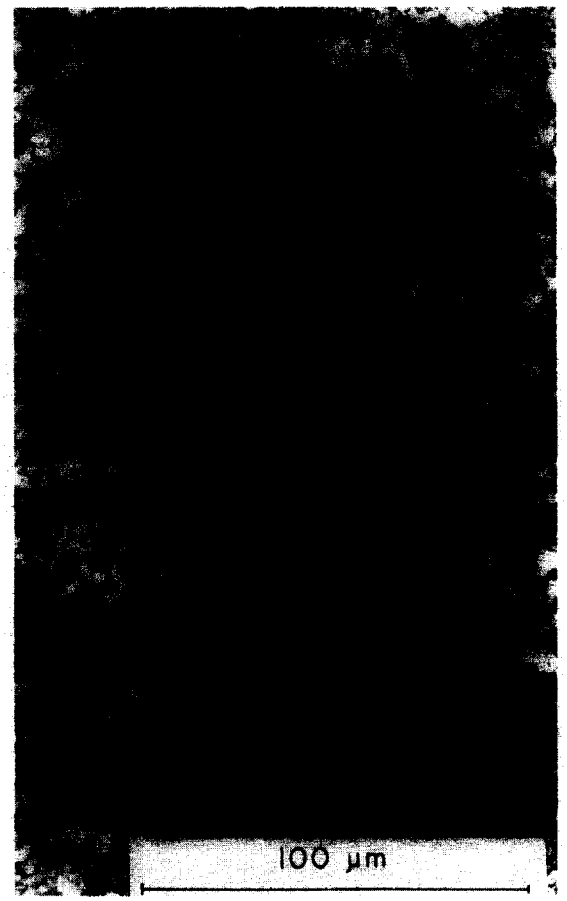

FIG. 3. Backscattered electron image of inclusion MX1/A. Dark gray hibonite is contained within lighter gray spinel. The slightly lighter shade of gray at the edges of spinel grains is due to increased iron concentration. Bright grains are perovskite or ilmenite.

is mantled by a discontinuous string of 1–2 μm sulfide grains (mostly troilite with some pentlandite). The important feature of MX1/D is that when all of the Ti in the analysis is reported as TiO_2, low cation sums are obtained. Analyses were recast into endmember components to calculate the amount of trivalent Ti. The fassaite is similar in composition to some fassaite found in Allende coarse-grained inclusions. The fraction $Ti^{3+}/(Ti^{3+} + Ti^{4+})$ obtained from four analyses are 0.45, 0.48, 0.51, 0.52, in good agreement with values found in Allende fassaite by HAGGERTY (1978) and BECKETT (1986). An analysis of coexisting spinel (Table 2) indicates no significant ferric iron content.

MX1 Matrix (Fig. 2a). Matrix silicates are difficult to analyze because of their small sizes. We managed to obtain nine good matrix olivine analyses: Fa 36 to Fa 49 (mean Fa 43). A few matrix pyroxene grains were encountered: Fs14/Wo8 (3.7% Al_2O_3), Fs12/Wo45 (0.9% Al_2O_3), Fs9/Wo39 (1.4% Al_2O_3). Matrix olivine is considerably more FeO-rich than the coexisting matrix pyroxene, a relationship also commonly observed in matrix olivine and pyroxene of type 3 ordinary chondrites (NAGAHARA, 1984; DODD, 1982). None of the matrix pyroxene contains ferric iron.

Some grains were encountered in MX1 matrix having oxide totals between 80 and 85 wt% (Table 4); they have analyses very similar to the analyses of "spinach" (layer-lattice silicate) reported by FUCHS *et al.* (1973) in Murchison. Most of these analyses contain minor sulfur; some have traces of sodium.

Table 2. Oxide minerals.

	1	2	3	4	5	6	7	8	9	10
MgO	0.94	11.69	4.20	0.47	14.53	2.34	0.66	13.02	20.62	15.19
Al_2O_3	87.15	62.81	1.24	3.55	63.93	4.06	5.62	61.53	55.42	52.46
SiO_2	0.55		0.15	0.19		0.34				
CaO	8.22		0.51	36.71			0.16	0.19		
TiO_2	1.48		51.67	54.42	0.25	26.33	1.73	0.36		
V_2O_3		0.23			0.24			0.53	0.35	
Cr_2O_3			0.56	0.29			27.93		14.39	15.15
MnO			1.01		0.23	1.21				
FeO	0.55	24.07	37.49	2.46	19.70	51.53	31.75	22.29	11.11	16.69
Fe_2O_3*		1.20	4.09		1.12	13.09	28.57			
Total	98.90	100.00	100.92	98.07	100.00	98.90	96.42	98.03	102.09	99.49
Atomic proportions										
Oxygens	19	4	3	3	4	4	4	4	4	4
Mg^{++}	0.158	0.464	0.151	0.016	0.565	0.127	0.037	0.524	0.788	0.615
Al^{+++}	11.612	1.971	0.035	0.096	1.966	0.174	0.251	1.957	1.675	1.679
Si^{++++}	0.062		0.004	0.004		0.012				
Ca^{++}	0.996		0.013	0.901			0.006	0.005		
Ti^{++++}	0.126		0.936	0.938	0.005	0.721	0.049	0.007		
V^{+++}		0.005			0.005			0.011	0.007	
Cr^{+++}			0.011	0.005			0.836		0.296	0.325
Mn^{++}			0.021		0.005	0.037				
Fe^{++}	0.052	0.536	0.755	0.047	0.430	1.569	1.006	0.503	0.238	0.379
Fe^{+++}		0.024	0.074		0.022	0.359	0.854			
Total	13.006	3.000	2.000	2.007	2.998	3.000	3.000	3.008	3.004	2.998

1. Hibonite in MX1/A. 2. Spinel in MX1/A. 3. Ilmenite in MX1/A. 4. Perovskite in MX1/A. 5. Spinel in MX1/B. 6. Titanomagnetite in MX1/B. 7. Chromian magnetite in MX1/C. 8. Spinel in MX1/D. 9. Spinel in MX4/A. 10. Spinel in MX4/B.
*Calculated from stoichiometry (*cf.* text).

Table 3. Pyroxenes.

	1	2	3	4	5	6
MgO	16.47	13.06	17.28	35.52	15.24	5.27
Al_2O_3	6.29	14.08	2.04	0.91	0.69	23.34
SiO_2	50.63	43.27	49.62	60.19	53.14	28.92
CaO	24.54	22.93	22.24	2.46	22.05	24.43
Ti_2O_3*						7.84
TiO_2	0.46	3.63	0.24			7.07
V_2O_3					0.27	
Cr_2O_3			0.63	0.43	0.83	0.36
FeO	1.17	1.87	2.02	2.32	7.55	0.81
Total	99.56	98.84	94.06	101.83	99.77	98.04
Cations per 6 oxygens						
Mg^{++}	0.893	0.719	0.996	1.765	0.844	0.305
Al^{+++}	0.270	0.613	0.093	0.036	0.030	1.067
Si^{++++}	1.842	1.598	1.918	2.006	1.975	1.122
Ca^{++}	0.957	0.907	0.921	0.088	0.878	1.015
Ti^{+++}						0.254
Ti^{++++}	0.013	0.101	0.007			0.206
V^{+++}					0.008	
Cr^{+++}			0.019	0.011	0.024	0.011
Fe^{++}	0.036	0.058	0.065	0.065	0.234	0.026
Total	4.010	3.995	4.019	3.970	3.994	4.006

1, 2. Fassaites in rim of MX1/A. 3. Diopside in rim of MX1/B. 4. Enstatite in MX1/C. 5. Salite in MX1/C. 6. Fassaite in MX1/D.
*Calculated from stoichiometry.

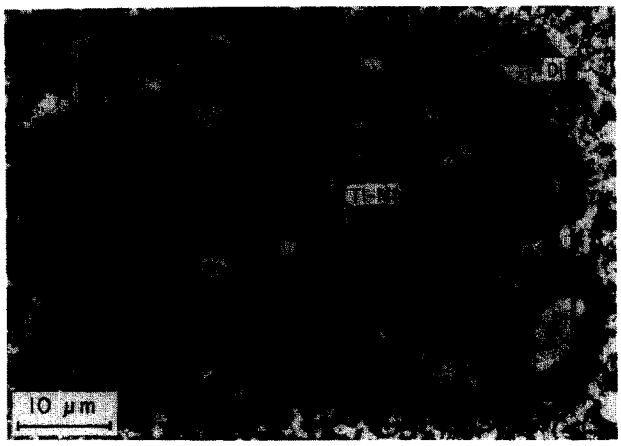

FIG. 4. Backscattered electron image of inclusion MX1/B, consisting largely of spinel (Sp) with some inclusions of perovskite (Pv) and titanomagnetite (Ti-Mt), and surrounded by a diopside (Di) rim.

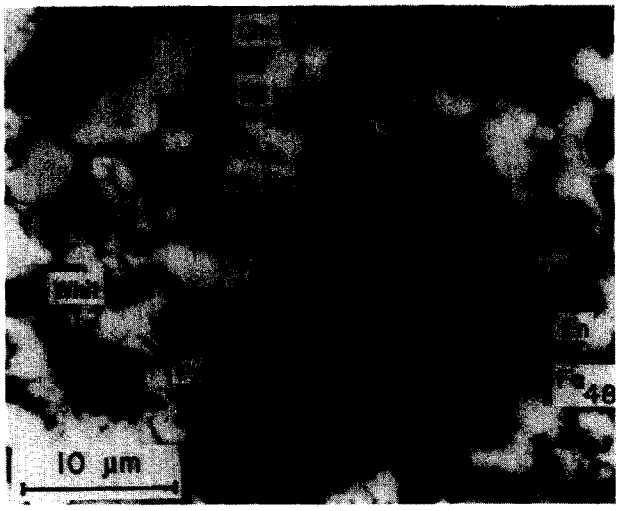

FIG. 6. Backscattered electron image of portion of MX1/C. Cr-rich magnetite (Chr) rims cores of Cr-poor magnetite (Mt). Pyroxene grains have cores of enstatite (En), mantles of Fe-bearing diopside (Di) and rims of Fe-rich olivine. Other minerals are discrete grains of whitlockite (Whit), metal (Ni-Fe) and pentlandite (Pn).

The presence of layer-lattice silicate in MX1 is confirmed by X-ray diffraction (*cf.* below).

MX2 (5.5 × 3.2 mm)

Thin section examination of MX2 reveals abundant opaque matrix, abundant sulfide (mainly troilite), and no metal, similar to MX1 and indicating it is a C3V subtype (VAN SCHMUS, 1969). A point count of the MX2 section gives a matrix/inclusion ratio of 1.5, also suggesting it is a C3V (MCSWEEN, 1977). No coarse grained rims around inclusions were seen, however, indicating it is a C3O (RUBIN, 1984). As with MX1, the matrix closely resembles the matrix of the type C3O, Ornans, at high magnification (10,000×). As with MX1, an unequivocal designation of subtype is not possible.

MX2 is separated from its host by a gypsum layer 15–20 μm thick. No gypsum occurs within the clast. This caused difficulty when MX2 was sampled for trace element analysis; the analysis shows anomalously high Ca because the gypsum layer could not be avoided when sampling (discussed later).

Inclusions in MX2 are much like those in MX1. Among them, one contained iron-rich spinel, titanomagnetite, ilmenite formed by alteration of perovskite, and minor amounts of nepheline and sodalite.

The matrix has a higher sulfide content than in MX1; troilite is more abundant than pentlandite. Matrix olivine grains are more FeO-rich (Fa38–41; Fa40 mean) than matrix pyroxene (Fs15–33), as in MX1. Repeated searches of the matrix failed to reveal any grains with "spinach"-like analyses, nor were there indications of phyllosilicates in X-ray diffraction patterns.

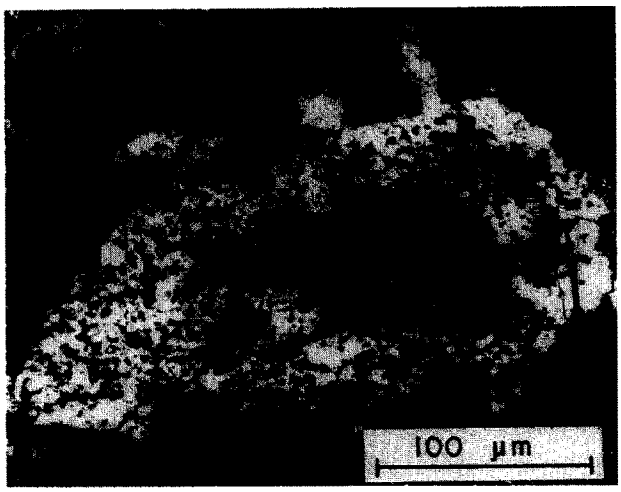

FIG. 5. Backscattered electron image of inclusion MX1/C. Bright grains of magnetite and pentlandite and dark gray grains of whitlockite surround a central area of dark gray calcic pyroxene grains.

FIG. 7. Backscattered electron image of inclusion MX1/D, an aggregate consisting mostly of fassaite (Fas) in the center, mostly spinel (Sp) around the outside, and a rim of pentlandite (Pn) and troilite (Tro).

Table 4. Phyllosilicate in MX1, "Spinach".

	1	2	3
MgO	16.89	19.95	16.14
Al_2O_3	5.20	1.77	4.03
SiO_2	30.69	30.63	28.81
CaO	0.59	0.27	1.04
FeO*	28.56	32.75	30.02
Total	81.93	85.36	80.05
Cations per 12 oxygens			
Mg^{++}	2.512	2.930	2.510
Al^{+++}	0.611	0.206	0.496
Si^{++++}	3.062	3.018	3.006
Ca^{++}	0.063	0.028	0.116
Fe^{++}	2.383	2.698	2.619
Total	8.632	8.880	8.747

*Total iron reported as FeO. This phase is known to have significant ferric iron content.

MX3 (2.3 × 1.6 mm)

This xenolith is dominated by a single porphyritic olivine (Fa 11–16) chondrule, 800 μm in diameter. The chondrule is surrounded by a very fine-grained, 100 μm thick rim of matrix that is nearly sulfide-free. Outside the rim is sulfide-rich matrix containing five moderately large mineral aggregates (165–350 μm) and many small mineral fragments. None of the aggregates is particularly remarkable. Each one, however, is high in iron; only rare grains have cores of more magnesian compositions. The silicates appear to have reacted extensively with an FeO-rich medium.

Single mineral fragments in the matrix are high in iron. One fragment (20 × 30 μm) is noteworthy. It shows three distinct zones that follow the irregular outline of its edge: the core is low-Ca pyroxene with a moderate FeO content (Fs13.0); this is surrounded by a Ca-pyroxene of similar FeO content (Fs15.2/Wo43.7); the outer edge is fayalitic olivine (Fa49.6).

The sulfide in the matrix is primarily troilite with minor pentlandite. Matrix olivine grains are Fa43–50 (Fa46 mean); only one matrix pyroxene gave a good analysis, Fs25/Wo32. No "spinach"-like compositions were found in the matrix.

MX4 (2 × 1.8 mm)

This xenolith contains a large olivine chondrule and a number of small aggregates. Seven aggregates were studied in detail. They present significant differences when compared to aggregates in all the other xenoliths. Five typical examples of these are described here.

Inclusion MX4/A (50 × 130 μm) consists of Cr-rich spinel (13.0–14.6% Cr_2O_3), olivine (Fa3.4–5.0), and minor Ca-pyroxene (Fs3.6). None of the silicate grains shows significant FeO enrichment at their edges. The Fe/(Fe + Mg) of one spinel grain varies from 0.084 to 0.233, center to edge, the edge abutting against a grain of low Fe-olivine, Fa3.4. The spinel stoichiometry indicates only ferrous iron is present (Table 2).

Inclusion MX4/B (150 × 200 μm) is a granular cluster of grains of olivine (Fa7.7) and low-Ca pyroxene (Fs4.3), both uniform in composition, and one grain of aluminous enstatite (Al_2O_3 = 16.38%, Fs8.7). A grain of Cr-rich (15.15%) spinel was found with a Fe/(Fe + Mg) ratio of 0.38. This spinel appears to have only ferrous iron (Table 2) similar to the spinel in inclusion MX4/A.

Inclusion MX4/C (170 × 200 μm) consists of granular fayalitic olivine, uniformly Fa44, with interstitial troilite, pentlandite and minor Al-rich chromite. The chromite appears to have only ferrous iron.

Inclusion MX4/D (250 × 370 μm) is an aggregate of granular, iron-poor olivine with interstitial troilite. Grains of olivine show significant FeO enrichment at their edges: *e.g.* Fa5.6 center, Fa11.5 edge.

Inclusion MX4/E (500 × 350 μm) consists of interlocking grains mainly of pyroxene (Wo1.1–1.2/Fs1.6–2.6) with lesser olivine (uniformly Fa5), interstitial troilite (6.9% Ni) and a single grain of metal (Ni = 5.6 mole%). FeO alteration has not affected any of the silicates in this inclusion.

MX4 matrix. Pyroxene grains in the matrix are more abundant than in the matrices of other MX clasts; the olivine/pyroxene ratio is about 2/1. Olivine has a mean composition of Fa47 and a fairly narrow range, Fa41–51. Matrix pyroxene has a large range in Fs content, 10–40, with Wo content of 2–6 (0–2.7% Al_2O_3); a single matrix grain of Ca-pyroxene was found (Wo38/Fs13). Again, as observed in the matrices

Table 5. Major and trace element abundances in MX1 and MX2.

Element	MX1		MX2	MX1/MX2*
	56.2 mg	1.950 mg	3.413 mg	
Na_2O (%)	0.704 ± .003	0.669 ± .005	0.565 ± .003	1.35
MgO (%)	21.4 ± 0.5	21.0 ± 0.9	23.5 ± 0.8	1.00
Al_2O_3 (%)	2.53 ± 0.04	2.59 ± 0.03	2.59 ± 0.03	1.10
K_2O (%)	0.0671 ± 0.0077	<0.099	0.07 ± 0.033	1.01
CaO (%)	2.18 ± 0.19	2.17 ± 0.30	5.61 ± 0.62	0.43
Sc (ppm)	9.53 ± 0.01	9.61 ± 0.01	12.07 ± 0.02	0.88
TiO_2 (%)	<0.15	<0.093	0.206 ± 0.049	<0.51
V (ppm)	77.7 ± 3.5	65.7 ± 3.6	74.2 ± 3.1	1.07
Cr (ppm)	3593 ± 6	5110 ± 100	2590 ± 50	1.87
Mn (ppm)	1894 ± 12	1570 ± 20	1980 ± 30	0.97
FeO (%)	32.40 ± 0.05	32.69 ± 0.05	28.36 ± 0.05	1.27
Co (ppm)	531 ± 1	689 ± 2	577 ± 3	1.17
Ni (%)	1.357 ± .009	1.529 ± 0.007	1.128 ± 0.006	1.42
As (ppm)	2.13 ± 0.23	1.44 ± 0.30	1.58 ± 0.26	1.25
Br (ppm)	—	0.82 ± 0.39	<0.40	
Se (ppm)	14.5 ± 0.3	28.8 ± 0.8	24.7 ± 0.5	0.97
Ru (ppm)	0.99 ± 0.20	0.79 ± 0.34	0.90 ± 0.39	1.10
Sb (ppb)	96 ± 13	149 ± 28	<49	
Cs (ppm)	<0.10	0.222 ± 0.052	<0.11	
La (ppb)	407 ± 11	403 ± 70	565 ± 62	0.80
Ce (ppm)	1.31 ± 0.21	<1.1	0.91 ± 0.26	1.58
Sm (ppb)	233 ± 4	217 ± 16	191 ± 11	1.31
Eu (ppb)	97.3 ± 4.2	97.2 ± 4.2	33.4 ± 4.3	3.23
Dy (ppb)	—	<480	<470	
Tm (ppb)	—	43 ± 17	49 ± 13	0.96
Yb (ppb)	317 ± 23	<310	260 ± 100	1.34
Lu (ppb)	22.6 ± 4.7	45 ± 12	56 ± 18	0.67
Hf (ppb)	99 ± 34	<160	66 ± 24	1.65
Ta (ppb)	<49	<55	<80	
Os (ppm)	0.957 ± 0.079	1.11 ± 0.18	1.20 ± 0.51	0.96
Ir (ppb)	713 ± 2	—	512 ± 4	1.53
Au (ppb)	171 ± 1	170 ± 7	88.5 ± 4.7	2.14

*Each normalized to respective MgO. MX1 values were averaged when two values were available.

of other MX xenoliths, pyroxene is much more magnesian than coexisting olivine.

Matrix sulfide is abundant, as in other MX xenoliths, and is mainly troilite with minor pentlandite. Some grains of pentlandite were found with cores of high Ni metal (Ni = 53–63 mole%).

Summary of petrographic observations

With respect to the criteria of VAN SCHMUS (1969) MX clasts are similar to C3O chondrites. Inclusion/matrix ratios and sizes of chondrule, aggregate and mineral fragments are like those of C3V chondrites in the two MX xenoliths (MX1 and MX2) large enough to make this measurement. The high sulfide contents are unique among C3 chondrites.

MX1 has inclusions with Fe^{3+}-bearing phases, indicating highly oxidizing conditions, and an inclusion with a Ti^{3+}-bearing phase, indicating highly reducing conditions. MX1 shows extensive FeO enrichment around the edges of silicates and alteration of perovskite to ilmenite, both indicating secondary reactions with an FeO-rich medium. MX1 has "spinach"-like phyllosilicates (*cf.* discussion below on phyllosilicates), which indicates hydrothermal reaction. MX2 and MX3 are similar to MX1, although MX3 appears to have undergone somewhat more extensive FeO enrichment, but with no indication of hydrous alteration. MX4 is quite different from the other three xenoliths; it has only rare iron enrichment and no indication of either ferric iron or hydrothermal reaction.

BULK PROPERTIES

Bulk chemical composition

Trace elements and some major and minor elements in MX1 and MX2 were determined by INAA (Table 5, Fig. 8).

Relative abundances of lithophile elements in MX1 do not consistently match those of any of the meteorite groups shown in Fig. 8, although the volatile lithophiles Mn, K and Na are closer to their mean abundances in C2 chondrites than to those of the other groups. For the siderophile and chalcophile elements, MX1 is generally enriched above all carbonaceous chondrite types in the more refractory elements Os, Ir, Ni and Fe. Exceptions are Co, which is normal, and Ru, whose uncertainty is large. At the more volatile end of this group of elements MX1 falls closest to C3O for some elements and C2 chondrites for others.

MX2 elemental data show more scatter than MX1, possibly as a result of its smaller sample size. Lithophile abundances in MX2 do not consistently match those of any of the meteorite groups shown in Fig. 8. Eu, V and Cr are strongly depleted relative to all of the carbonaceous chondrite types. Ca in MX2 appears to be greatly enriched relative to all carbonaceous chondrites (Table 5; not plotted in Fig. 8). This is an artifact due to the fact that MX2, as described earlier, is surrounded by a layer of gypsum separating it from the surrounding Murchison host. There was no way to avoid collecting gypsum during sampling. The gypsum apparently does not affect the other trace element abundances. If it did we would predict Se, which follows S, to be greatly enriched over MX1, which is not the case (Table 5, col. 4). For the siderophile and chalcophile elements MX2 is generally closer to the C3V chondrites, but Os and Se are higher, and Sb and Au lower than in all other C2 and C3 chondrite types.

In summary, these two xenoliths are not identical: MX1 is higher in most trace elements than MX2 (Table 5, col. 4).

Oxygen isotopes

The bulk oxygen isotopic compositions of MX1 and MX2 are distinct from each other and from the Murchison host:

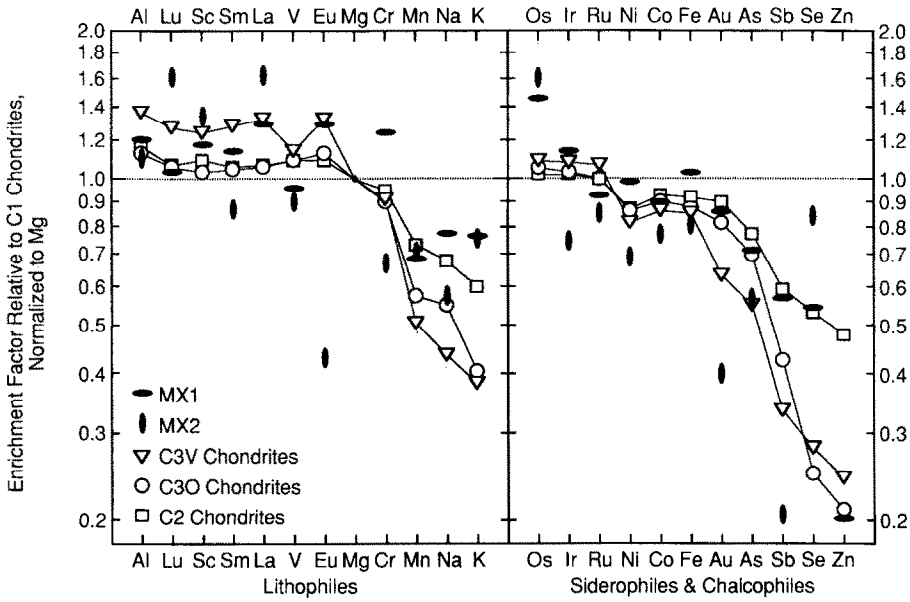

FIG. 8. C1 chondrite-normalized elemental abundance pattern of bulk MX1 and MX2 compared to those of mean C2, C3O, and C3V chondrites. The data for the latter three groups are from KALLEMEYN and WASSON (1981). All abundances are normalized to MgO to correct for differences in concentration of highly volatile elements.

MX1 has $\partial^{17}O = -1.42$ per mil and $\partial^{18}O = +4.12$ per mil; MX2 has $\partial^{17}O = +0.45$ per mil and $\partial^{18}O = +6.13$ per mil. Within their respective errors they lie along a line (Fig. 9) that contains bulk Murchison (point B), Murchison anhydrous concentrate (point A), Murchison phyllosilicate concentrate (point M). Point B is not truly representative of bulk Murchison; CLAYTON and MAYEDA (1984) note there is a significant difference in reactivity between phyllosilicate (very reactive) and refractory phases (less reactive) to the chemical treatment that liberates bulk oxygen. Since Murchison consists of about half of each of these major components (ANDERS, 1964, 1968, 1971; LARIMER and ANDERS, 1967; L. GROSSMAN and OLSEN, 1974), the point for bulk Murchison should lie half way between the points A and M. The lower reactivity of refractory phases causes the measured point to lie about three-fourths of the way toward the more reactive phyllosilicate concentrate point, M.

Neither MX1 nor MX2 plot within the group of C3 chondrites that lie along the Allende refractory inclusion line (Fig. 9). The Murchison refractory inclusion line passes through point A, paralleling the Allende line, even farther from the two MX points. The MX points are, however, not unique. Point LV-2, a xenolith in Leoville (KRACHER *et al.*, 1985), and point PV-B1, a xenolith in Plainview (WILKENING and CLAYTON, 1974) plot close to MX2 (Fig. 9). LV-2 is slightly hydrously altered and PV-B1 is a C2 chondrite (Table 1).

From these data it is apparent there are meteoritic objects with distinct oxygen isotopic compositions, including MX1 and MX2, that are both hydrous and anhydrous. The degree of hydrous alteration is not a discriminating factor. The oxygen isotopic composition must have been acquired by these objects independently. Clearly, MX1 and MX2 do not represent degrees of interaction with the Murchison host, otherwise hydrously altered MX1 should lie closer to point M than anhydrous MX2.

Carbon, nitrogen, sulfur

Total carbon and $\partial^{13}C$ were measured on samples from MX1 and MX2. MX1 has C = 1074 ppm and $\partial^{13}C$ (PDB) = −17.0 per mil, MX2 has C = 4619 ppm and $\partial^{13}C$ (PDB) = −16.7 per mil. MX1 contains 1959 ppm S and 145 ppm N; MX2 contains 3293 ppm S and 1560 ppm N. The samples used to determine these compositions were collected from the centers of the xenoliths. This avoided the contamination of the gypsum rim around MX2 that occurred when larger samples were collected for INAA.

In a plot of $\partial^{13}C$ *vs.* $\partial^{18}O$ (WRIGHT *et al.*, 1988) MX1 and MX2 plot close together, and widely separated from the field of C1 and C2 chondrites. They are clearly not related to these groups. On the $\partial^{13}C$ *vs.* total C plot of KERRIDGE (1985), both MX points lie within the C3 field. These carbon data confirm the association of MX1 and MX2 with C3 chondrites. The factor of four higher C in MX2, relative to MX1, indicates these two clasts do not have the same origin.

In Kerridge's plot of bulk N *vs.* bulk C, however, MX1 plots in the C3 cluster while MX2 plots by itself in an unpopulated portion of the diagram, with a total nitrogen content characteristic of C1 chondrites. Neither the site nor the chemical state of nitrogen in these chondrites is known. Nitrogen in MX2 is enriched by a factor of two above the Murchison host (KERRIDGE, 1985). Although Kerridge's data show some scatter in bulk nitrogen for individual C3 chondrites, none of the data show sufficient scatter to encompass the enrichment found in MX2. The nitrogen data again confirm the MX1 association with the C3 group; however, MX2 has an unusual nitrogen content, well above that of the Murchison host rock (KUNG and CLAYTON, 1978). MX2 must have acquired its nitrogen prior to incorporation into the Murchison host. Similarly, MX1 did not acquire much nitrogen from the Murchison host, which has a nitrogen concentration six times that of MX1 (KERRIDGE, 1985). The bulk nitrogen data reinforce the evidence from the carbon data that MX1 and MX2 originated from different sources.

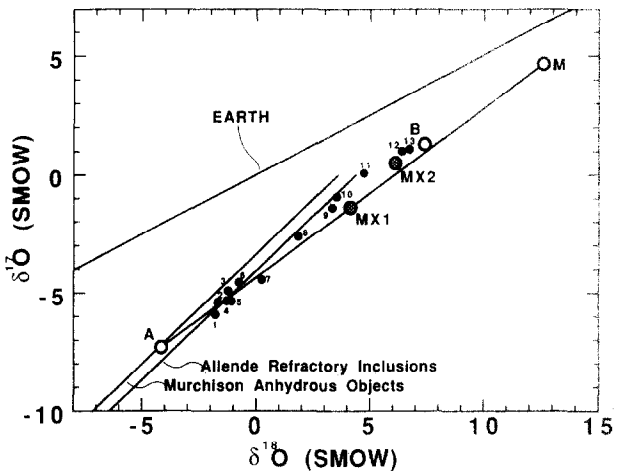

FIG. 9. Oxygen three-isotope plot. The points are marked: A—Murchison anhydrous phases concentrate; B—Murchison bulk; M—Murchison hydrous phyllosilicate concentrate; 1—Kainsaz (C3O); 2—Ornans (C3O); 3—Lancé (C3O); 4—Coolidge (C4); 5—Karoonda (C5); 6—Warrenton (C3O); 7—Vigarano (C3V); 8—Allende (C3V); 9—Grosnaja (C3V); 10—Mokoia (C3V); 11—Bali (C3V); 12—Plainview xenolith, PV-B1; 13—Leoville xenolith, LV-2.

The 68% higher S content in MX2 than MX1 confirms our petrographic observation of a significantly higher sulfide mineral content. Earlier we observed that all MX xenoliths appear petrographically richer in sulfide minerals, principally troilite, than other C3 chondrites. Bulk sulfur contents measured in MX1 and MX2 are, however, a factor of 7–10 lower than the average of C3 chondrites (SCHNEIDER, 1978; MOORE, 1971). The conclusion to be drawn from these data is that much sulfur in C3 chondrites (presumably as sulfide) is present as submicrometer grains in the matrix, where it is not visible. If these xenoliths were ever average C3 chondrites, their sulfides must have been recrystallized into larger, more visible grains, with significant loss of total sulfur. This suggests that these xenoliths have undergone some thermal metamorphism prior to their emplacement into the hydrous Murchison host, which contains approximately ten times more total sulfur than either MX1 or MX2. Clearly, these xenoliths did not interact significantly with the host with respect to sulfur.

Phyllosilicate(s) in MX1

As noted earlier, some matrix grains in MX1 give analyses (Table 4) that are very similar to analyses of Murchison phyllosilicates (Fuchs *et al.*, 1973) and to analyses of phyllosilicates

in the Vigarano C3V chondrite (BUNCH and CHANG, 1980). All of the MX clasts were large enough for bulk X-ray powder diffraction and all show the expected diffraction peaks for olivine, pyroxene and sulfide; however, MX1 has, in addition, peaks at 7.0, 3.60, and 1.70 Å, which are characteristic of the berthierine phyllosilicates (BARBER, 1981). TOMEOKA and BUSECK (1983a,b), COHEN and KORNACKI (1983), BUNCH and CHANG (1980), KRACHER *et al.* (1985) and HASHIMOTO and GROSSMAN (1987) have reported phyllosilicates in C3 meterorites, however, they have not been noted as significant phases, sufficient to generate observable diffraction peaks in bulk meteorite samples. Experiments using mixtures of phyllosilicate-rich Orgueil and phyllosilicate-free Ornans indicate that phyllosilicates must be present at the $\approx$10 wt% level before they can be detected by X-ray diffraction.

The infrared spectra of MX1 and five carbonaceous chondrites with a variety of bulk water contents: Allende, Murchison, Orgueil, Ornans, and Vigarano, show an absorption peak due to OH stretching at $\approx$3500 cm^{-1}. This peak is broad and has contributions from mineral hydroxyl groups and adsorbed water. The OH peak was recorded in the absorbance mode and the peak area measured for each sample. The area was plotted *vs.* literature analyses of total water in the five bulk meteorites and an excellent linear correlation was found. The spectrum of MX1 contains a small OH peak, similar in size to that of our blank. From the plot we infer it contains <2 wt% water.

To determine the water content better, MX1 was also analyzed for hydrogen using an ion microprobe. The H^+ count rate from MX1 matrix was approximately one tenth that obtained from Murchison matrix analyzed concurrently, indicating that MX1 contains $\approx$1 wt% water. This result agrees with the amount of phyllosilicate estimated from the X-ray diffraction pattern.

To investigate phyllosilicate formation, a series of simple experiments was performed. Powdered charges of bulk Allende were sealed in gold foil tubes containing excess water and heated in Morey bombs under two sets of conditions: T = 300°C, $P(H_2O)$ = 500 bars for 48 hours; and T = 200°C, $P(H_2O)$ = 15 bars for 35 days. Both run products showed strong, sharp 7 Å lines. Phyllosilicates presumably formed from the fayalitic olivine laths making up the Allende matrix (Fig. 2c). Similar results were obtained from an experiment using a small slice of Allende, 1 × 2 × 2 mm, reacted at T = 300°C, $P(H_2O)$ = 500 bars for 72 hours. Excavation into the center of the slice revealed that physllosilicate had formed, demonstrating that the porosity is sufficient to allow significant penetration by water vapor. Two additional experiments were performed on powdered Allende at lower temperatures and pressures to attempt to estimate the minimum conditions required to form phyllosilicates from fayalitic olivine: T = 80°C, $P(H_2O)$ = 0.5 bars for 6 months; and at room temperature using liquid water for 8 years. Neither experiment produced detectable phyllosilicates.

Experimental data for the hydrothermal reaction of fayalitic olivine to form layer-lattice silicates are sparse. MOODY (1976) investigated the serpentinization of olivine (Fa7) (products: serpentine + ferroan brucite + magnetite) over the range of 0.6 to 2 kbars water pressure. He found a (pseudo) univariant reaction curve parallel to the iron-free curve (forsterite + water = serpentine + brucite) and 14°C lower in temperature. JANECKY and SEYFRIED (1986) obtained significant alteration of synthetic oceanic peridotite with sea water at 500 bars and 200°C to 300°C with run durations of 4 hours to 2 years. They found that the reaction rates of olivine, enstatite and diopside were in the proportions 3/10/2, in moles per unit time per unit surface area. Their olivine, orthopyroxene and diopside compositions were more iron-rich than those of Moody (1976).

These simple experiments demonstrate that the matrix phases of Allende, dominantly submicrometer grains of olivine averaging around Fa50 (Fig. 2c), can be altered to some kind(s) of hydrous phyllosilicate(s). Oxidation may also play a role; matrix phyllosilicates in C2 meteorites appear to be, in part, made up of ferric chamosites (FUCHS *et al.*, 1973). KRACHER *et al.* (1985) observed that hydrous alteration affects fine-grained matrix materials first.

DISCUSSION

There are only three logical environments in which these xenoliths could have undergone their different degrees of alteration: (1) in the nebula; (2) within the Murchison parent body; (3) within their own parent body, or parent bodies.

Alteration in the nebula

If all these xenoliths underwent alteration by reaction with a well mixed nebular gas, we would predict the degree and kind of alteration would be the same for all of them. PECK and WOOD (1987) concluded that the uniform FeO enrichment at the edges of olivine grains in Allende resulted from reaction with a dry, FeO-rich nebular gas at relatively high temperature. HUA *et al.* (1987) came to the same conclusion based on their study of FeO-rich edges of olivine grains in Grosnaja and Allende.

Differences between the Murchison xenoliths in FeO alteration, degree of partial oxidation and reaction with water indicate the alteration environment was not homogeneous. Furthermore, in all cases in which interaction with a nebular medium is suspected, the oxygen isotopic composition of different objects lie on a line of unit slope, which is not the case for MX1 and MX2.

Alteration in the Murchison parent body

The fact that MX2, which is not hydrously altered, has an oxygen isotopic composition closer to the phyllosilicate point M (Fig. 9) than MX1, which *is* hydrously altered, means that these two xenoliths could not have acquired their oxygen isotopic compositions simply by interaction with the Murchison host. Also, large differences in the nitrogen, carbon and sulfur contents of MX1 and MX2 cannot have been acquired by reaction with Murchison.

In addition, INAA data show that MX1 has a bulk Fe/Mg ratio significantly greater than that of Murchison and nearly all C2 and C3 chondrites surveyed by KALLEMEYN and WASSON (1981, 1982). Only Renazzo has a similar high Fe/Mg ratio. Because MX1 has a higher Fe/Mg ratio than Murchison, it is highly unlikely that the Murchison host is the source of the excess iron in this xenolith. MX2, on the other hand, is depleted in total iron relative to both MX1 and the Murchison host.

Refractory lithophile and siderophile element abundances are generally higher in MX1 than in mean C2 chondrites and Murchison. With few exceptions, volatile element abundances in MX1 are closest to those in mean C2 chondrites and Murchison, and are higher than those in either C3 subtype. The simple conclusion one might draw from these data is that the more volatile components, including water, may have been homogenized between Murchison and MX1. Sulfur, nitrogen and carbon, on the other hand, were not homogenized. Volatile element abundances in MX2 are often depleted relative to those in Murchison, suggesting that significant homogenization of volatiles and water did not take place in MX2, although iron addition was more extensive than in MX1. The differences in trace elements between MX1 and MX2 could not have been achieved by simple interaction with the Murchison host.

Finally, it might be argued that the hydrous alteration of MX1 could reflect much longer residence time in the Murchison parent body relative to the other xenoliths. Oxygen isotopic differences with MX2 do not support this, as stated above. It could be argued, however, that the present oxygen isotopic compositions of these two xenoliths represent initial differences prior to their incorporation into Murchison and that the oxygen isotopic composition of MX1 was then modified by reaction with water from the Murchison host. It is possible to assess the factor of hydrothermal reaction kinetics on the formation time of phyllosilicates based on our hydrothermal experiments, described earlier.

WOOD and WALTHER (1983) showed that hydrothermal reaction rates are independent of both the type of reaction and the partial pressure of water. They are dependent primarily on temperature and a moderate to high pH (>7). The pH of pore water in rock depends on the minerals in contact with the water. The minerals that make up the bulk of the Murchison xenoliths are olivine and pyroxene. These minerals create pH values of 10 to 11 (STEVENS, 1934; STEVENS and CARRON, 1948). Using Eqns. (4) and (5) of Wood and Walther it is possible to make an estimate of the time required for the same degree of partial alteration to phyllosilicate at 25°C, as occurred in our lowest temperature successful experiment (200°C, 35 days). The estimate is of the order of 200 to 300 years. A similar calculation (based on the same successful experiment: 200°C, 35 days) for the attempted reaction at 80°C (no phyllosilicates in 6 months) indicates significant reaction would occur in about 10 years. These calculations also suggest that at the temperatures derived in the model of CLAYTON and MAYEDA (1984), <20°C, hydration processes that lead to the development of abundant phyllosilicates can occur on a reasonable time scale of a few hundred years.

Thus, kinetic factors within the stability field of phyllosilicates cannot account for the lack of phyllosilicate in MX2, MX3 and MX4. If MX2 and MX3 were altered *in situ* sufficiently to enrich edges of mineral grains in their inclusions with iron, and to oxidize some ferrous iron to ferric iron, significant phyllosilicate development would have taken place.

We conclude that alteration of the Murchison xenoliths was not the result of significant interaction with the Murchison host.

CONCLUSIONS

Based on the foregoing discussion, we conclude that the MX xenoliths did not acquire their significant alteration features within the Solar nebula or by reaction within the Murchison host but, rather, prior to their incorporation into Murchison.

The scenario of essentially closed system hydrous alteration proposed by DUFRESNE and ANDERS (1962), and more recently developed in detail by TOMEOKA and BUSECK (1985), must have affected the Murchison parent body prior to the incorporation of the MX xenoliths, otherwise the xenoliths would all show significant development of phyllosilicates. Given the temperature and water content to effect the changes observed in the Murchison host rock, the xenoliths would all have to have been significantly hydrothermally altered. The kinetics are very favorable for this kind of reaction (WOOD and WALTHER, 1983).

The development of secondary phases in the Murchison xenoliths requires at least two episodes of alteration: (1) Ferrous iron enrichment, with or without some oxidation to ferric iron, coupled with Fe-Mg exchange; (2) low temperature hydrous alteration. The episodes appear unrelated judging from the lack of correlation between degree of iron enrichment, phyllosilicate content and the oxygen isotopic composition.

The Murchison xenoliths, like the "Blue Angel" in Murchison (ARMSTRONG *et al.*, 1982), underwent individual alteration histories prior to accretion into the Murchison parent body. This appears to have happened in their one or more parent bodies.

Acknowledgements—We thank J. R. Goldsmith and R. C. Newton for valuable aid in performing the hydrothermal experiments, R. W. Hinton for making the ion microprobe measurements, and V. Ekambaram for a portion of the neutron activation analyses. We thank G. J. MacPherson and R. C. Newton for useful discussions. The infrared spectrophotometry was done in the Materials Research Laboratory of the University of Chicago (funded by National Science Foundation grant DMR 82-16892). This research was supported by grants from the National Science Foundation, EAR 83-16812 (R.N.C.) and the National Aeronautics and Space Administration, NAGW-23 (E.O.); NCL 14-001-169 (R.N.C.); NAG 9-111 (A.M.D.); and NGR 14-001-249 and NAG 9-54 (L.G.). Additional support was received from the Chalmers Fund of the Field Museum of Natural History.

Editorial handling: W. R. Van Schmus

REFERENCES

ANDERS E. (1964) Origin, age, and composition of meteorites. *Space Sci. Rev.* **3**, 583–714.

ANDERS E. (1968) Chemical processes in the early solar system, as inferred from meteorites. *Acc. Chem. Res.* **1**, 289–298.

ANDERS E. (1971) Meteorites and the early solar system. *Ann. Rev. Astron. Astrophys.* **9**, 1–34.

ARMSTRONG J. T., MEEKER G. P., HUNEKE J. C. and WASSERBURG G. J. (1982) The Blue Angel: 1. The mineralogy and petrogenesis of a hibonite inclusion from the Murchison meteorite. *Geochim. Cosmochim. Acta* **46**, 575–595.

BANNER A. E. and STIMPSON B. P. (1975) A combined ion probe/spark source analysis system. *Vacuum* **24**, 511–517.

BARBER D. (1981) Matrix phyllosilicates and associated minerals in

C2M carbonaceous chondrites. *Geochim. Cosmochim. Acta* **45**, 945–970.

BECKETT J. R. (1986) The origin of Ca-, Al-rich inclusions from carbonaceous chondrites: An experimental study. Ph.D. dissertation, Univ. of Chicago, 373p.

BINNS R. A. (1967) Farmington meteorite: cristobalite xenoliths and blackening. *Science* **156**, 1222–1226.

BISCHOFF A. and KEIL K. (1983) Ca-Al-rich chondrules and inclusions in ordinary chondrites. *Nature* **303**, 588–592.

BISCHOFF A., KEIL K. and STÖFFLER D. (1985) Perovskite-hibonite-spinel-bearing inclusions and Al-rich chondrules and fragments in enstatite chondrites. *Chem. Erde* **44**, 97–106.

BUNCH T. E., CHANG S., NEIL J. M. and BURLINGAME A. (1976) Unique characteristics of the Jodzie howardite. *Meteoritics* **11**, 260–261.

BUNCH T. E. and CHANG S. (1980) Carbonaceous chondrites—II. Carbonaceous chondrite phyllosilicates and light element geochemistry as indicators of parent body processes and surface conditions. *Geochim. Cosmochim. Acta* **44**, 1543–1577.

CHRISTOPHE MICHEL-LEVY M. C. and CURIEN H. (1965) Étude à la microsonde électronique d'un chondre d'olivine et d'un fragment riche en cristobalite de la météorite de Nadiabondi. *Bull. Soc. Fr. Mineral. Cristogr.* **88**, 122–125.

CLAYTON R. N. and MAYEDA T. K. (1963) The use of bromine pentafluoride in the extraction of oxygen from oxides and silicates for isotopic analysis. *Geochim. Cosmochim. Acta* **27**, 43–52.

CLAYTON R. N. and MAYEDA T. K. (1984) The oxygen isotope record in Murchison and other carbonaceous chondrites. *Earth Planet. Sci. Lett.* **67**, 151–161.

COHEN R. E. and KORNACKI A. S. (1983) Mineralogy and petrology of chondrules and inclusions in the Mokoia CV3 chondrite. *Geochim. Cosmochim. Acta* **47**, 1739–1757.

DODD R. T. (1974) Petrology of the St. Mesmin chondrite. *Contrib. Mineral. Petrol* **46**, 129–145.

DODD R. T. (1982) *Meteorites: A Petrologic-Chemical Synthesis.* Cambridge Univ. Press, 368p.

DUFRESNE E. R. and ANDERS E. (1962) On the chemical evolution of the carbonaceous chondrites. *Geochim. Cosmochim. Acta* **26**, 1085–1114.

EL GORESY A., NAGEL K. and RAMDOHR P. (1978) Fremdlinge and their noble relatives. *Lunar Planet. Sci. Conf. 9th* 1279–1303.

FODOR R. V. and KEIL K. (1976) Carbonaceous and non-carbonaceous lithic fragments in the Plainview, Texas chondrite: Origin and history. *Geochim. Cosmochim. Acta* **40**, 177–189.

FUCHS L. H., OLSEN E. and JENSEN K. J. (1973) Mineralogy, mineral-chemistry, and composition of the Murchison (C2) meteorite. *Smithson. Contrib. Earth Sci. No. 10*, 39p.

GROSSMAN L. and OLSEN E. (1974) Origin of the high-temperature fraction of C2 chondrites. *Geochim. Cosmochim. Acta* **38**, 173–187.

GROSSMAN L., OLSEN E., DAVIS A. M., TANAKA T. and MACPHERSON G. J. (1981) The Antarctic achondrite ALHA 76005: A polymict eucrite. *Geochim. Cosmochim. Acta* **45**, 1267–1279.

HAGGERTY S. E. (1978) The Allende meteorite: evidence for a new cosmothermometer based on Ti^{3+}/Ti^{4+}. *Nature* **276**, 221–225.

HALBOUT J., MAYEDA T. K. and CLAYTON R. N. (1986) Carbon isotopes and light element abundances in carbonaceous chondrites. *Earth Planet. Sci. Lett.* **80**, 1–18.

HASHIMOTO A. and GROSSMAN L. (1987) Alteration of Al-rich inclusions inside ameoboid olivine aggregates in the Allende meteorite. *Geochim. Cosmochim. Acta* **51**, 1685–1704.

HUA X., ADAM J., PALME H. and EL GORESY A. (1987) Fayalite-rich rims around forsteritic olivines in CAIs and chondrules in carbonaceous chondrites: Types, compositional profiles and constraints of their formation. *Lunar Planet. Sci. XVIII*, 443–444.

HUTCHISON R., WILLIAMS C. T., DIN V. K., PAUL R. L. and LIPSCHUTZ M. E. (1986) An achondritic troctolite clast in the Barwell, L5-6, chondrite. *Meteoritics* **21**, 402–403.

JANECKY D. R. and SEYFRIED W. E. JR. (1986) Hydrothermal serpentinization of peridotite within the oceanic crust: Experimental investigations of mineralogy and major element chemistry. *Geochim. Cosmochim. Acta* **50**, 1357–1378.

KALLEMEYN G. W., BOYNTON W. V., WILLIS J. and WASSON J. T. (1978) Formation of the Bencubbin polymict meteoritic breccia. *Geochim. Cosmochim. Acta* **42**, 507–515.

KALLEMEYN G. W. and WASSON J. T. (1981) The compositional classification of chondrites I. The carbonaceous chondrite groups. *Geochim. Cosmochim. Acta* **45**, 1217–1230.

KALLEMEYN G. W. and WASSON J. T. (1982) The compositional classification of chondrites III. Ungrouped carbonaceous chondrites. *Geochim. Cosmochim. Acta* **46**, 2217–2228.

KERRIDGE J. F. (1985) Carbon, hydrogen and nitrogen in carbonaceous chondrites: Abundances and isotopic compositions in bulk samples. *Geochim. Cosmochim. Acta* **49**, 1707–1714.

KRACHER A., KEIL K., KALLEMEYN G. W., WASSON J. T., CLAYTON R. N. and HUSS G. I. (1985) The Leoville (CV3) accretionary breccia. *Proc. Lunar Planet. Sci. Conf. 16th, Part 1; J. Geophys. Res.* **90**, D123–D135.

KUNG C-C and CLAYTON R. N. (1978) Nitrogen abundances and isotopic compositions in stony meteorites. *Earth Planet. Sci. Lett.* **38**, 421–435.

KURAT G., PALME H., BRANDSTÄTTER F. and HUTH H. (1987) Allende-AF: Undisturbed record of condensation, accretion, and metasomatism. *Lunar Planet. Sci. VIII*, 523–524.

LARIMER J. W. and ANDERS E. (1967) Chemical fractionation in meteorites—II. Abundance patterns and their interpretation. *Geochim. Cosmochim. Acta* **31**, 1239–1270.

MAYEDA T. K., CLAYTON R. N. and YANAI K. (1986) Oxygen isotopic compositions of several Antarctic meteorites. *Mem. Natl. Inst. Polar Res., Special Issue* **46**, 144–150.

MCSWEEN H. Y. JR. (1977) Carbonaceous chondrites of the Ornans type: A metamorphic sequence. *Geochim. Cosmochim. Acta* **41**, 477–491.

MIYAMOTO M. H., TAKEDA H. and YANAI K. (1979) Eucritic polymict breccias from Allan Hills and Yamato Mountains, Antarctica. *Lunar Planet. Sci. X*, 847–849.

MOODY J. B. (1976) An experimental study on the serpentinization of iron-bearing olivines. *Can. Mineral.* **14**, 462–478.

MOORE, C. B. (1971) Sulfur (16). In *Handbook of Elemental Abundances in Meteorites* (ed. B. MASON) pp. 137–142, Gordon & Breach Sci. Publ., New York.

NAGAHARA H. (1984) Matrices of type 3 ordinary chondrites—primitive nebular records. *Geochim. Cosmochim. Acta* **48**, 2581–2595.

NOZETTE S. and WILKENING L. L. (1982) Evidence for aqueous alteration in a carbonaceous xenolith from the Plainview (H5) chondrite. *Geochim. Cosmochim. Acta* **46**, 557–563.

OLSEN E., NOONAN A., FREDRIKSSON K., JAROSEWICH E. and MORELAND G. (1978) Eleven new meteorites from Antarctica. *Meteoritics* **13**, 209–225.

OLSEN E., MAYEDA T. K. and CLAYTON R. N. (1981) Cristobalite-pyroxene in an L6 chondrite: Implications for metamorphism. *Earth Planet. Sci. Lett.* **56**, 82–88.

OLSEN E., DOD B. D., SCHMITT R. A. and SIPIERA P. (1987) Monticello: A glass-rich howardite. *Meteoritics* **22**, 81–97.

PECK J. A. and WOOD, J. A. (1987) The origin of ferrous zoning in Allende chondrule olivines. *Geochim. Cosmochim. Acta* **51**, 1503–1510.

RAMBALDI E. R. and RAJAN R. S. (1982) Evidence for primitive phosphates in highly unequilibrated ordinary chondrites (abstr.). *Meteoritics* **17**, 271–272.

RUBIN A. (1984) Coarse-grained chondrule rims in type 3 chondrites. *Geochim. Cosmochim. Acta* **48**, 1779–1789.

RUBIN A., SCOTT E. R. D. and KEIL K. (1982) Microchondrule-bearing clast in the Piancaldoli LL3 meteorite: a new kind of type 3 chondrite and its relevance to the history of chondrules. *Geochim. Cosmochim. Acta* **46**, 1764–1776.

RUBIN A., SCOTT E. R. D., TAYLOR G. J., KEIL K. and ALLEN J. S. B. (1983) Nature of the H chondrite parent body regolith: Evidence from the Dimmitt breccia. *Proc. Lunar Planet. Sci. Conf. 13th, Part 2*, A741–A754.

RUBIN A. E. and GROSSMAN J. N. (1985) Phosphate-sulfide assemblages and Al/Ca ratios in type-3 chondrites. *Meteoritics* **20**, 479–489.

SCHNEIDER A. (1978) Sulfur abundance in cosmos, meteorites, tektites

and lunar materials. In *Handbook of Geochemistry* (ed. K. H. WEDEPOHL), 11-2, Part 16-C. Springer-Verlag, Berlin.

STEELE I. M., HERVIG R. L., HUTCHEON I. E. and SMITH J. V. (1981) Ion microprobe techniques and analysis of olivine and low-Ca pyroxene. *Amer. Mineral.* **66,** 526–546.

STEVENS R. E. (1934) Studies on the alkalinity of some silicate minerals. *U.S. Geol. Surv. Paper 185A,* 1–13.

STEVENS R. E. and CARRON M. K. (1948) Simple field test for distinguishing minerals by abrasion pH. *Amer. Mineral.* **33,** 31–49.

TAYLOR G. J., MAGGIORE P., SCOTT E. R. D., RUBIN A. and KEIL K. (1987) Original structures, and fragmentation and reassembly histories of asteroids: Evidence from meteorites. *Icarus* **69,** 1–13.

TOMEOKA K. and BUSECK P. R. (1983a) An exotic Fe-Ni-S-O layered mineral: An improved characterization of the "poorly characterized phase" in C2M carbonaceous chondrites (abstr.). *Lunar Planet. Sci. XIV,* 789–790. Lunar Planet. Inst., Houston.

TOMEOKA K. and BUSECK P. R. (1983b) Unusual microstructures in the C2 carbonaceous chondrites. *Nature* **299,** 327–329.

TOMEOKA K. and BUSECK P. R. (1985) Indicators of aqueous alteration in CM carbonaceous chondrites: microtextures of a layered mineral containing Fe, S, O, and Ni. *Geochim. Cosmochim. Acta* **49,** 2149–2163.

VAN SCHMUS W. R. (1969) Mineralogy, petrology, and classification of types 3 and 4 carbonaceous chondrites. In *Meteorite Research* (ed. P. MILLMAN) Reidel, Dordrecht.

WILKENING L. L. (1973) Foreign inclusions in stony meteorite—I. Carbonaceous chondritic xenoliths in the Kapoeta howardite. *Geochim. Cosmochim. Acta* **37,** 1985–1989.

WILKENING L. L. and CLAYTON R. N. (1974) Foreign inclusion in stony meteorites—II. Rare gases and oxygen isotopes in a carbonaceous chondrite xenolith in the Plainview gas-rich chondrite. *Geochim. Cosmochim. Acta* **38,** 937–945.

WOOD B. J. and WALTHER J. V. (1983) Rates of hydrothermal reactions. *Science* **222,** 413–415.

WRIGHT I. P., GRADY M. M. and PILLINGER C. T. (1988) Carbon, oxygen and nitrogen isotopic compositions of possible martian weathering products in EETA 79001. *Geochim. Cosmochim. Acta* **52,** 917–924.